

Supplemental online materials to:

MEL-18 loss mediates estrogen receptor- α downregulation and hormone independence

Jeong-Yeon Lee¹, Hee-Young Won², Ji-Hye Park¹, Hye-Yeon Kim², Hee-Joo Choi², Dong-Hui Shin², Ju-Hee Kang³, Jong-Kyu Woo⁴, Seung-Hyun Oh⁴, Taekwon Son⁵, Jin-Woo Choi², Sehwan Kim⁶, Hyung-Yong Kim^{2, 6}, Kijong Yi², Ki-Seok Jang², Young-Ha Oh², Gu Kong^{1, 2, *}

¹Institute for Bioengineering and Biopharmaceutical Research (IBBR), Hanyang University, Seoul, Republic of Korea

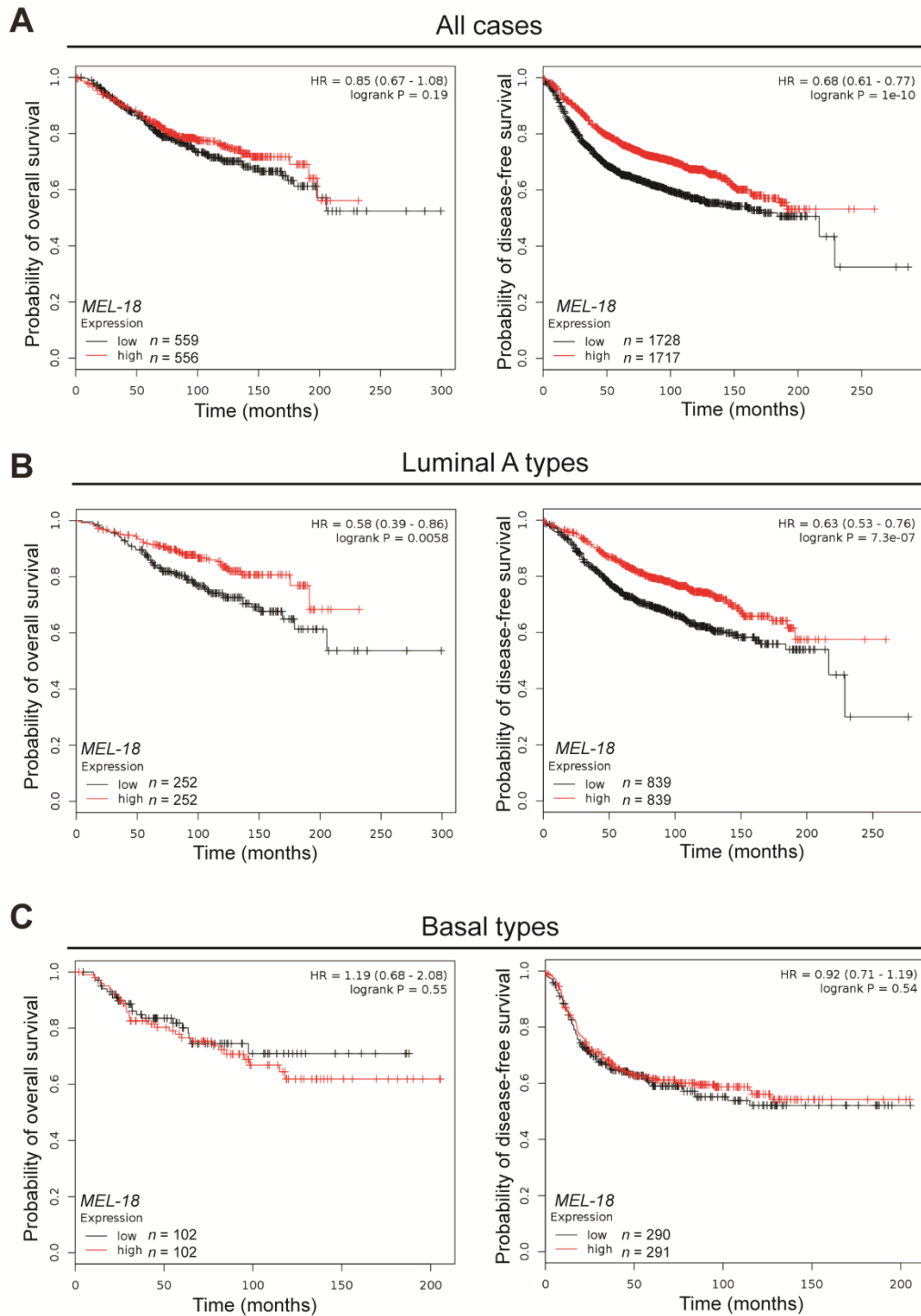
²Department of Pathology, College of Medicine, Hanyang University, Seoul, Republic of Korea

³National Cancer Center, Goyang-si, Gyeonggi-do, Republic of Korea

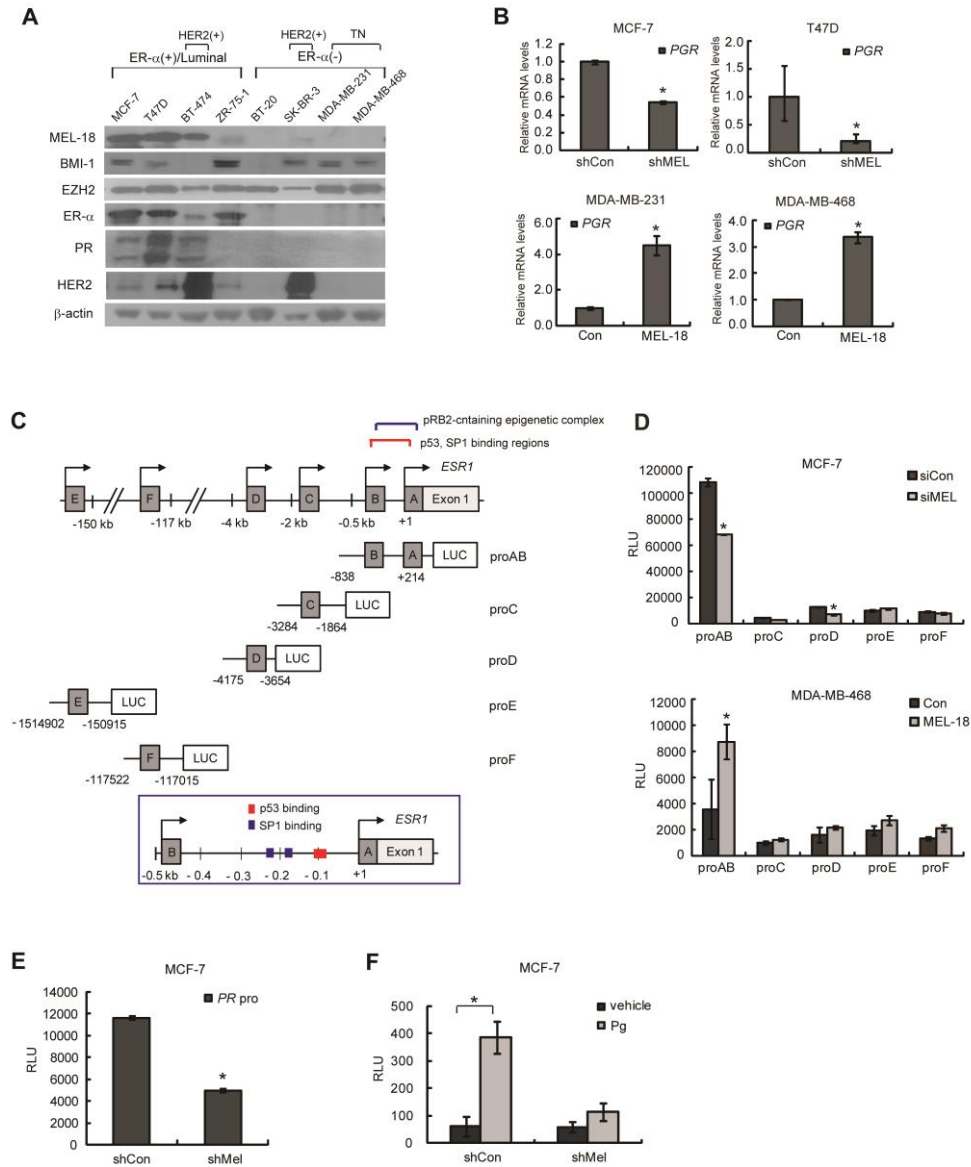
⁴College of Pharmacy, Gachon University, Incheon, Republic of Korea

⁵Research Institute, Bio-Medical Science Co., Ltd., Daejeon, Republic of Korea

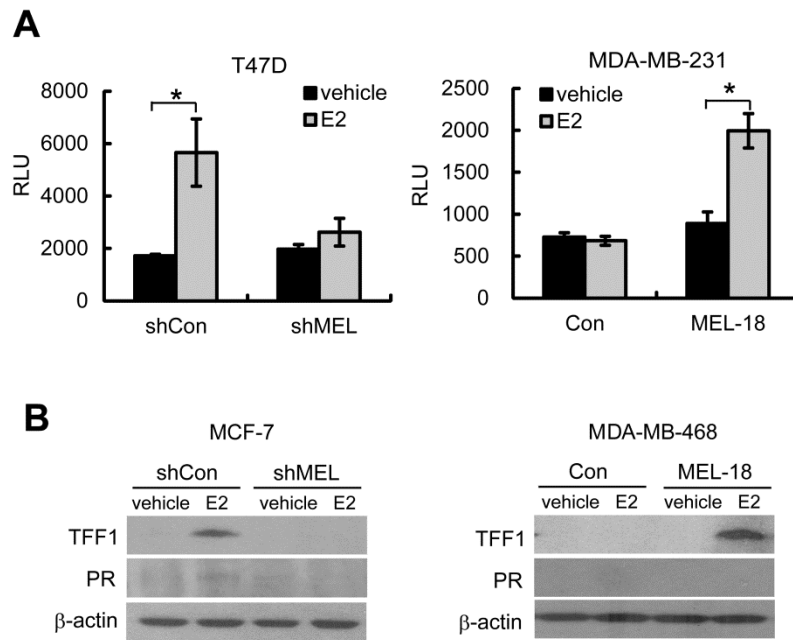
⁶Data Science Center, Insilicogen, Inc., Suwon-si, Gyeonggi-do, Republic of Korea



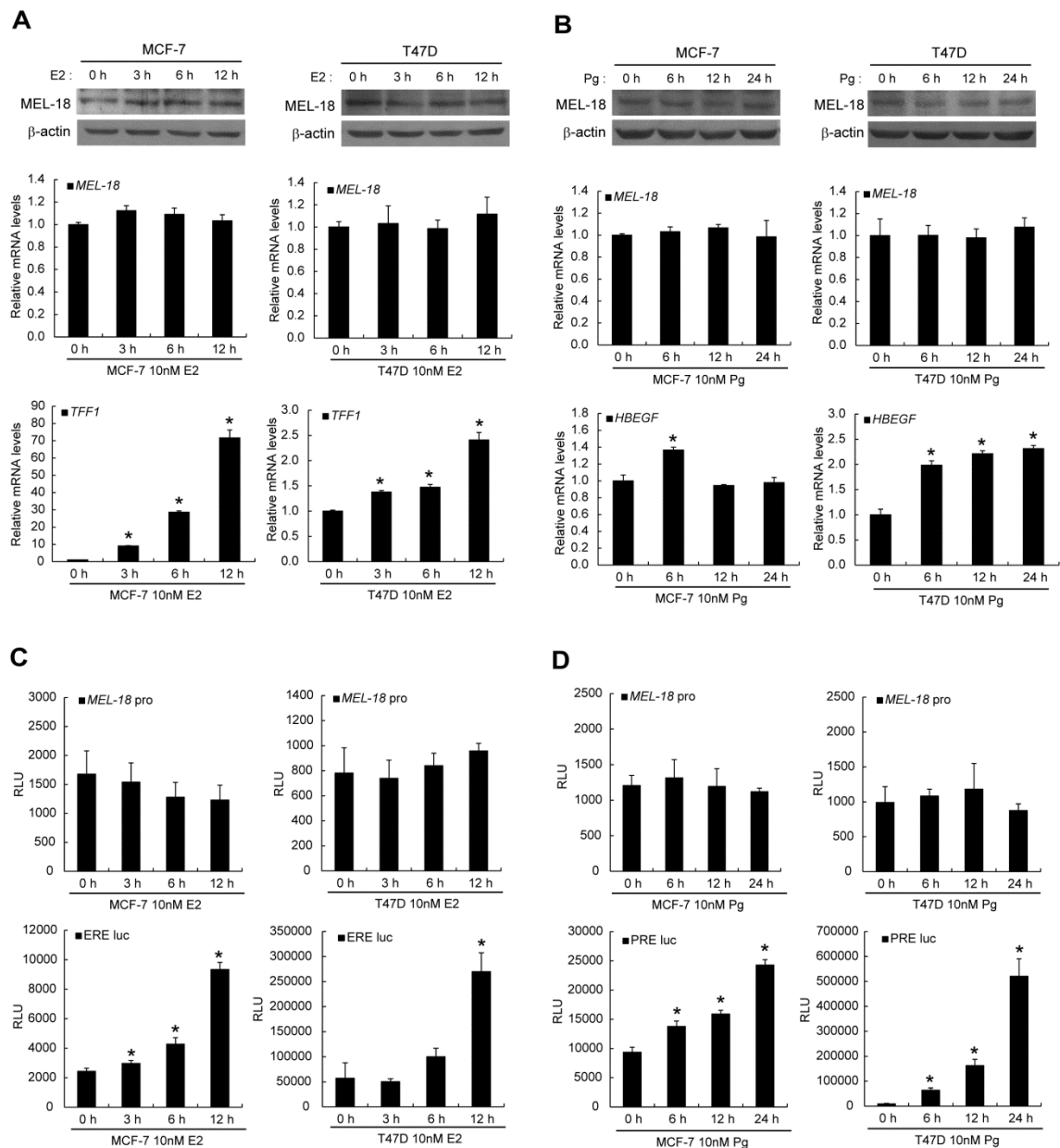
Supplemental Figure 1 Clinical relevance of *MEL-18* expression in the human breast cancer cohorts. (A-C) The OS and DFS of the indicated subtypes of breast cancer patients according to *MEL-18* mRNA expression levels was analyzed using Kaplan-Meier Plotter (<http://kmplot.com/analysis>).



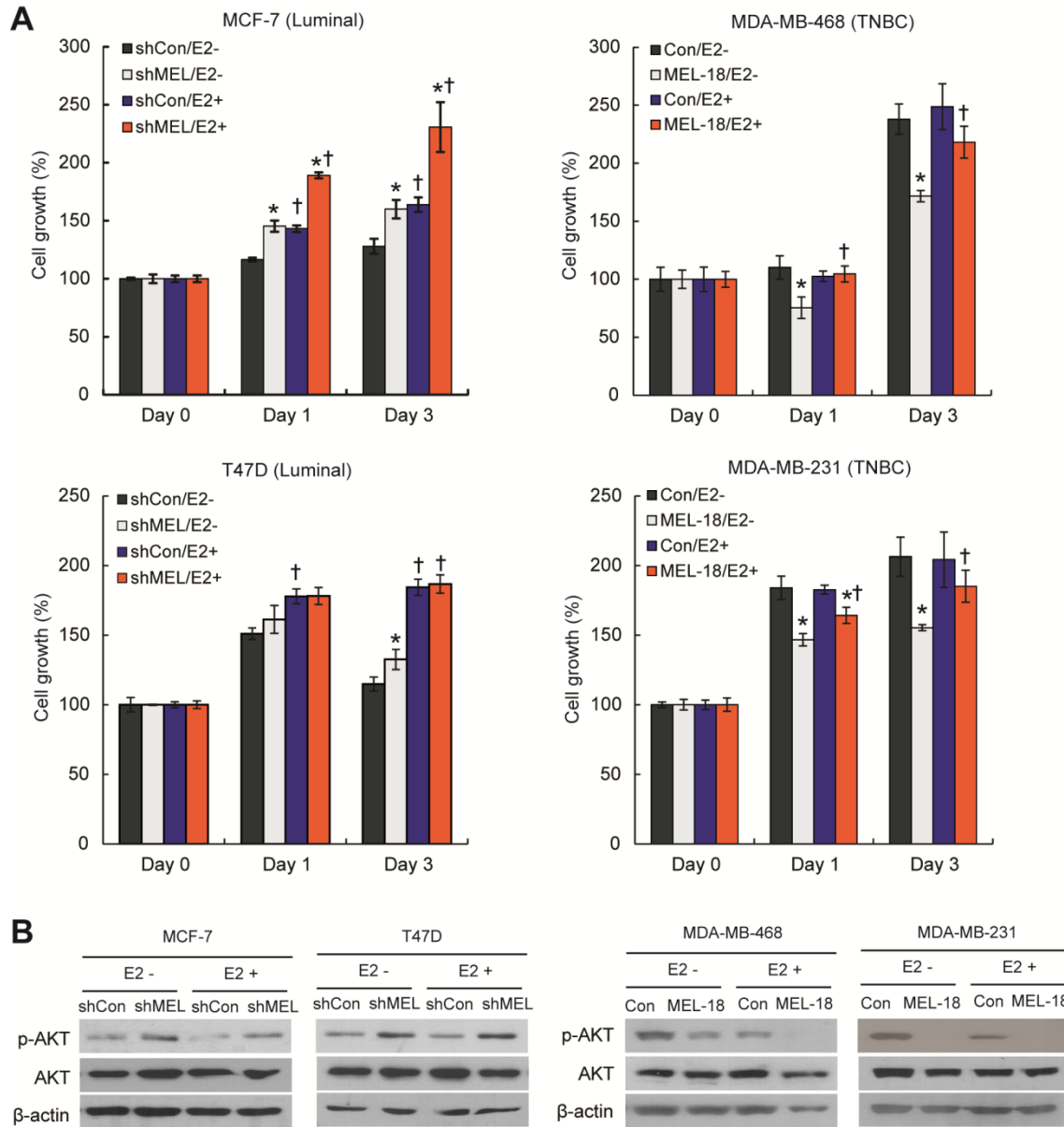
Supplemental Figure 2 The effect of MEL-18 on hormone receptor transcription and activity. **(A)** Immunoblotting of lysates from breast cancer cell lines to determine the expression of the indicated proteins. β -actin was used as a loading control. **(B)** The mRNA levels of *PR* (*PGR*) in MCF-7 cells expressing either control (shCon) or MEL-18 shRNA (shMEL) were validated by qRT-PCR. **(C)** Schematic illustration of the promoter regions of the human *ESR1* gene locus and the promoter fragments of *ESR1* cloned into the luciferase reporter vector as previously described (1). The blue and red lines indicate the previously described binding regions of the transcription factors and the epigenetic modulators of *ESR1* transcription (top) (2-4). The binding regions of p53 and SP1 in the proximal promoter of *ESR1* are presented (bottom). **(D)** Luciferase reporter assays of *ESR1* promoter activity in MCF-7 cells transiently transfected with control (siCon) or MEL-18 siRNA (siMEL) or MDA-MB-468 cells transiently transfected with empty vector (Con) or MEL-18 cDNA. **(E)** The effect of MEL-18 on PR transcription. Luciferase reporter assays were used to measure *PR* promoter activity in MEL-18-silenced MCF-7 cells. **(F)** PRE luciferase assay of control and MEL-18-silenced MCF-7 cells in the presence or absence of 10 nM R5020, a synthetic progesterone (Pg), for 24 h. The error bars in B and D-F represent the means \pm SD of triplicate experiments. * $P < 0.05$ compared to the controls (shCon, siCon, or Con) based on a 2-tailed Student's *t* test.



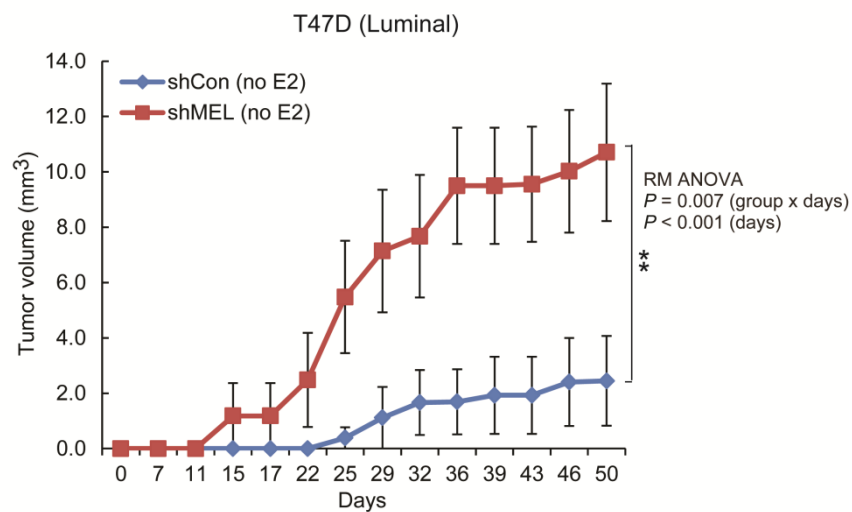
Supplemental Figure 3 The effect of MEL-18 on hormone receptor activity. **(A)** ERE luciferase activity was measured in the indicated cell lines in the presence or absence of 10 nM E2 for 24 h. The error bars represent the means \pm SD of triplicate samples. $*P < 0.05$ versus the controls (shCon or Con) based on a 2-tailed Student's *t* test. **(B)** Immunoblotting for TFF1 (also known as pS2) and PR expression in control, MEL-18-silenced (left), or MEL-18-overexpressing (right) cells in the presence or absence of E2 (10 nM in MCF-7 cells or 20 nM in MDA-MB-468 cells) for 24 h. Parallel samples examined on separate gels are shown. The data shown are representative of three independent experiments.



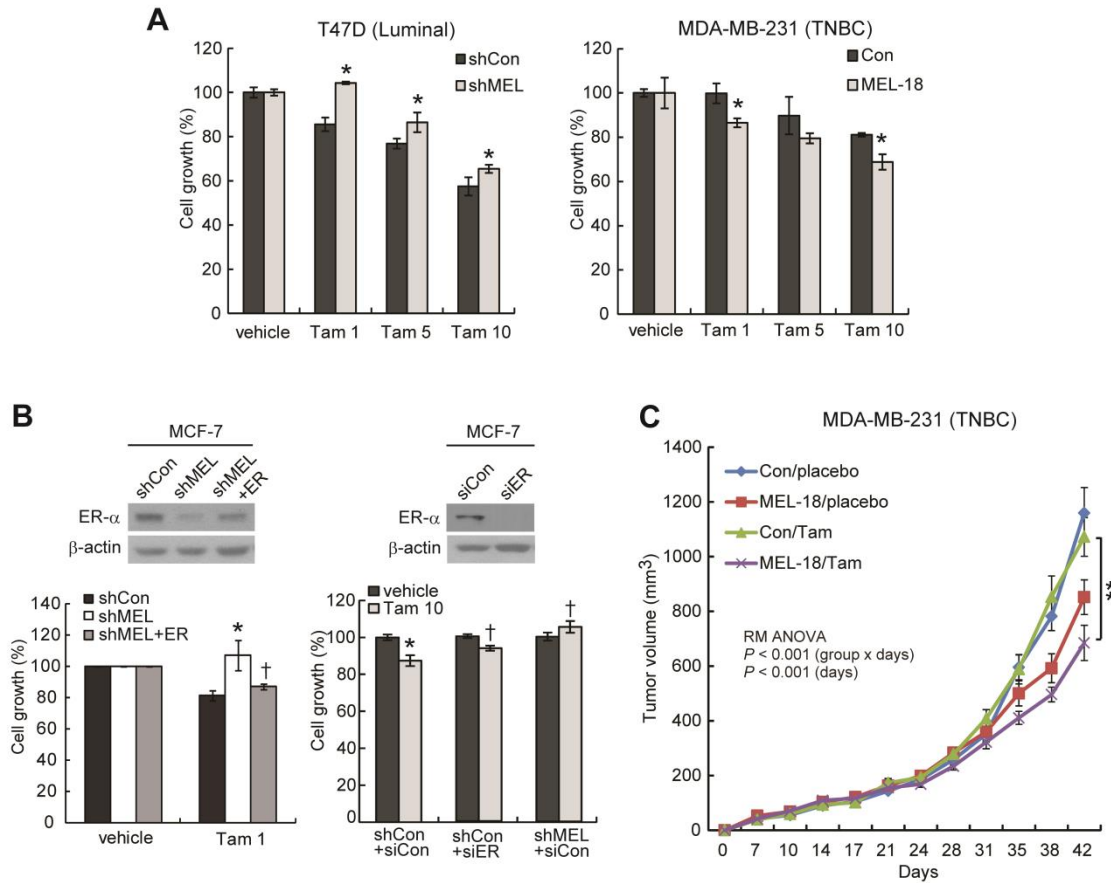
Supplemental Figure 4 The effect of hormone activity on MEL-18 expression. (A-D) Cells were treated with 10 nM E2 (A and C) or 10 nM synthetic progestin (Pg) R5020 (B and D) for the indicated periods and subjected to immunoblotting (A and B, top), qRT-PCR (A and B, bottom), or a *MEL-18* promoter activity assay (C and D). *TFF1* and ERE-luc or *HG-EGF* and PRE-luc were used as positive controls for E2- and R5020-induced activities, respectively. The error bars represent the means \pm SD of triplicate samples. * $P < 0.05$ compared to the control (0 h) based on a 2-tailed Student's *t* test.



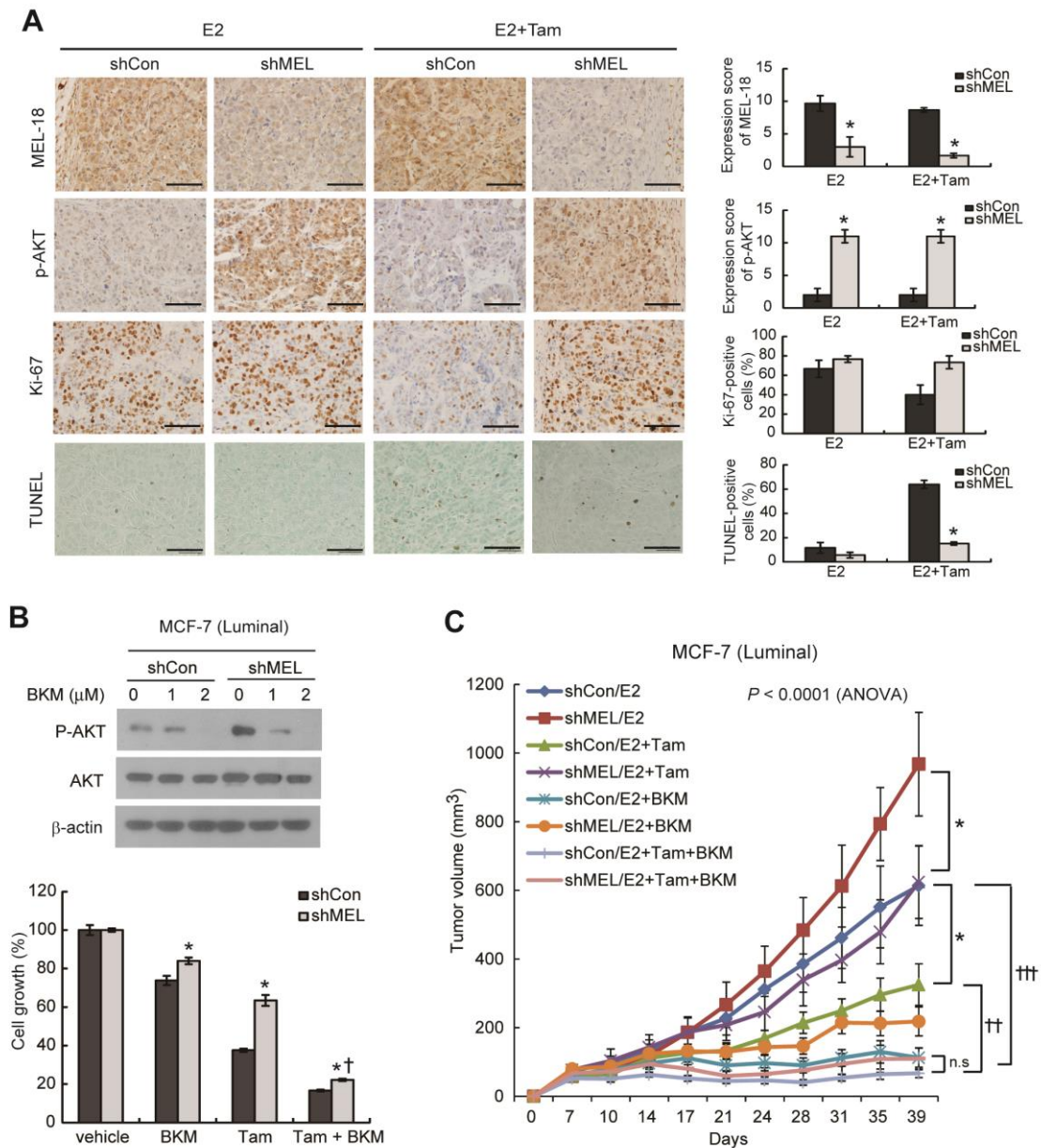
Supplemental Figure 5 The effect of MEL-18 on the estrogen response of breast cancer cells. (A) Cells were treated with either 10 nM E2 or ethanol (vehicle), and cell growth was analyzed by MTT assay. The results are presented as the means \pm SD of triplicate experiments. * and †, $P < 0.05$ compared to the control (shCon or Con) and vehicle (E2-), respectively (2-tailed Student's t test). (B) AKT activity in the indicated cell lines treated with or without E2 for 48 h was measured via immunoblotting using an anti-phospho-AKT antibody.



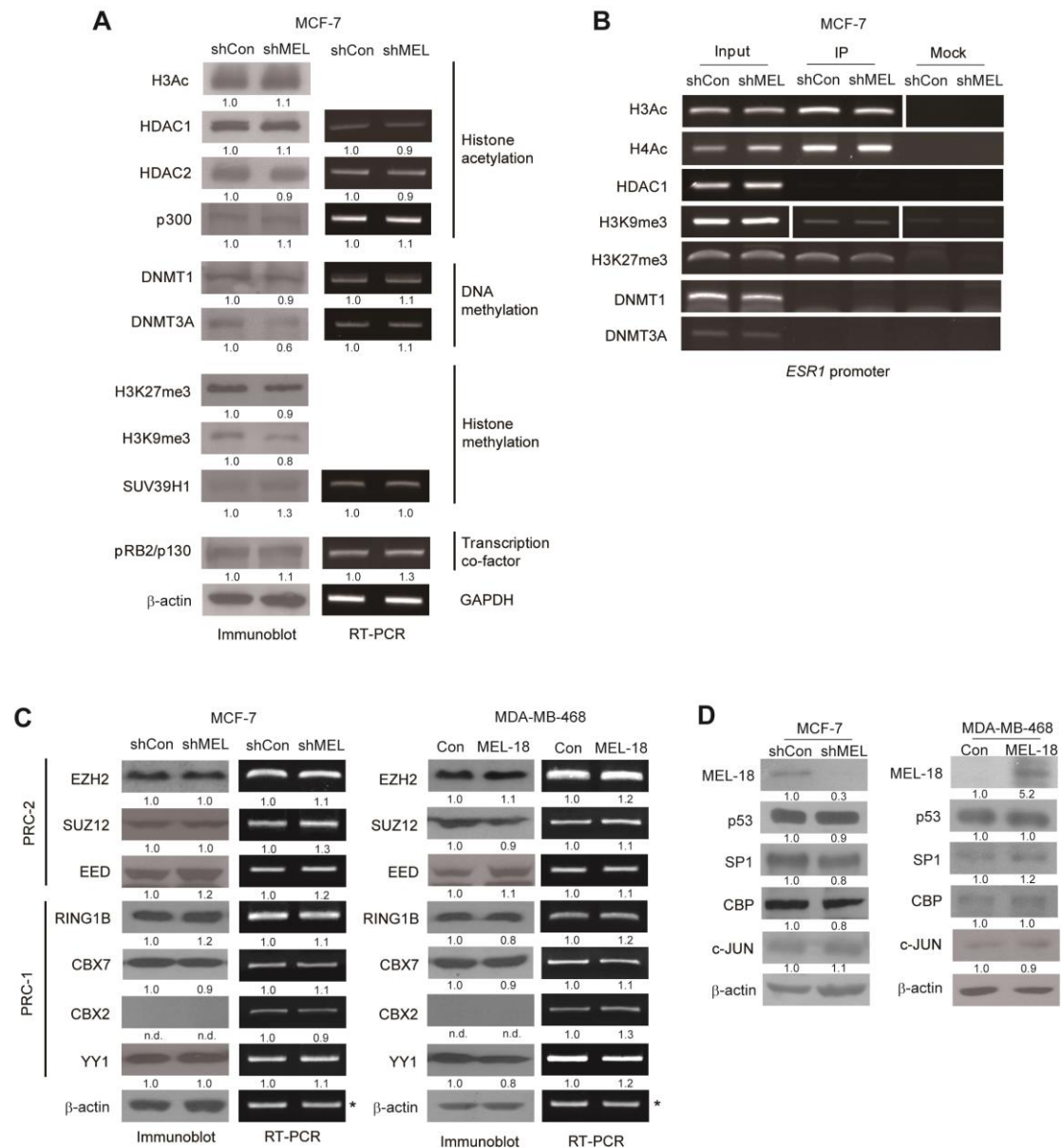
Supplemental Figure 6 The effect of MEL-18 depletion on estrogen-independent T-47D breast tumor growth in vivo. T47D cells expressing either control (shCon) or MEL-18 shRNA (shMEL) were transplanted into the mammary fat pads of NOD/SCID mice ($n = 8$) in the absence of E2 pellet injection. The tumor size was monitored for 8 wk to analyze tumor growth in the xenografted mice. The data are presented as the means \pm SEM. ** $P < 0.01$ (group x days) based on RM ANOVA.



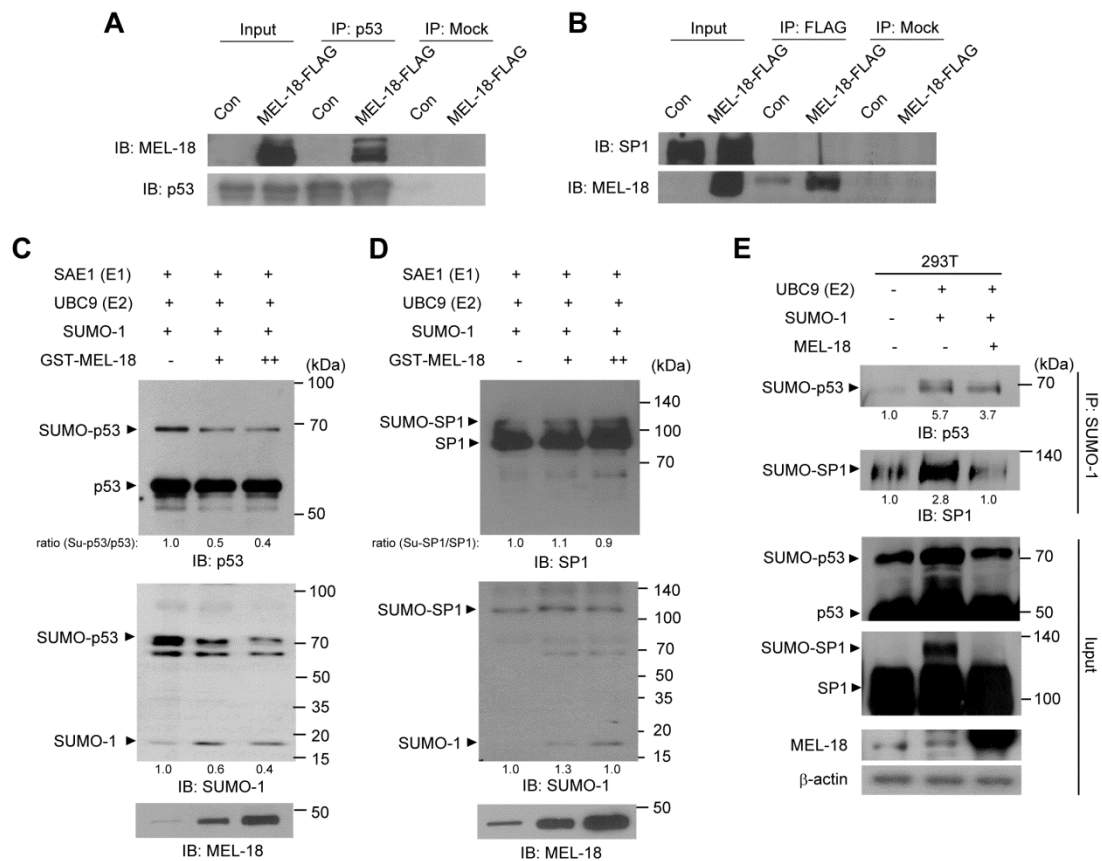
Supplemental Figure 7 The effect of MEL-18 on the response of breast cancer cells to tamoxifen. (A) Cells were treated with the indicated doses (μ M) of tamoxifen (Tam) or ethanol (vehicle) for 5 d, and cell growth was analyzed via the MTT assay. The data are presented as the means \pm SD of triplicate experiments. * $P < 0.05$ versus shCon or Con (2-tailed Student's t test). (B) After the generation of MEL-18-silenced MCF-7 cells stably expressing ER- α , the growth of these cells treated with 1 μ M tamoxifen for 5 d was analyzed via the MTT assay (left). Control or MEL-18-silenced MCF-7 cells transfected with either control (siCon) or ER- α siRNA (siER) were treated with 10 μ M tamoxifen for 3 d (right) and subjected to the MTT assay. The error bars represent the means \pm SD ($n = 3$). (C) Xenografted mice bearing control (Con) or MEL-18-overexpressing MDA-MB-231 cell-based tumors were implanted with either tamoxifen (Tam) or placebo to analyze the effect of MEL-18 on the response of TNBC cells to tamoxifen in vivo ($n = 8$ per groups). The tumor size was monitored for 42 d. The data are presented as the means \pm SEM. $P < 0.001$ (days), $P < 0.001$ (group x days) based on RM ANOVA. ** $P = 0.003$, Con/Tam versus MEL-18/Tam (post hoc LSD test).



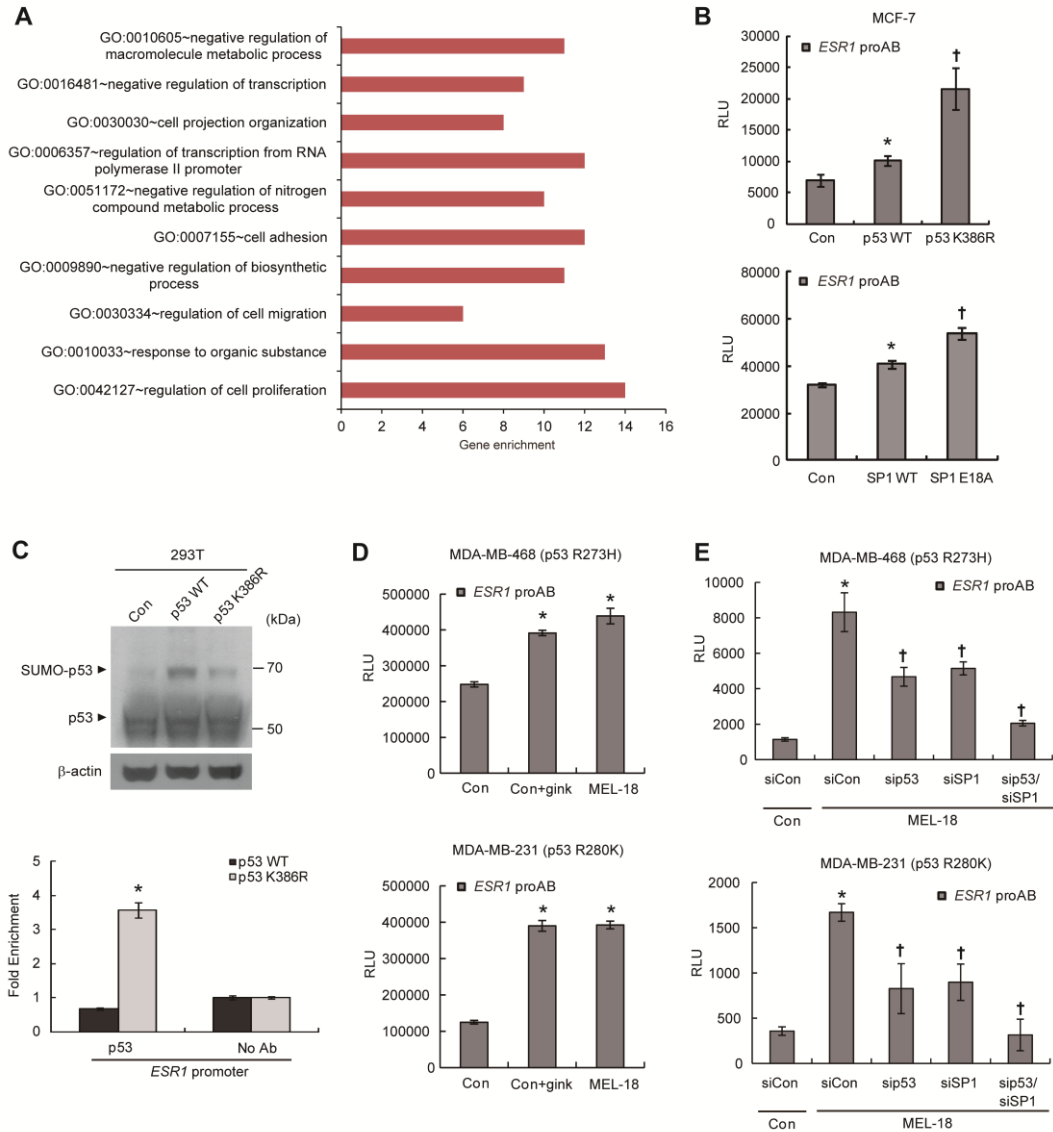
Supplemental Figure 8 The effect of AKT activity on the MEL-18-mediated regulation of the tamoxifen response. **(A)** IHC analysis of phosphorylated AKT to analyze the effect of MEL-18 on AKT activity in vivo (upper). Ki-67 and TUNEL assays for the in vivo analysis of cell proliferation and apoptosis, respectively, in the indicated samples (lower). **(B)** The cells were treated with 10 μM tamoxifen, 1 μM BKM120 (BKM), or both for 48 h and were subjected to the MTT assay. The error bars represent the means ± SD of triplicate measurements. * $P < 0.05$ versus shCon; † $P < 0.05$ versus Tam (2-tailed Student's t test). **(C)** Xenografted mice bearing control or MEL-18-silenced MCF-7 cell-based tumors injected with E2 pellets were administered tamoxifen, BKM, or both ($n = 5$ for the E2 and E2+Tam groups; $n = 8$ for the E2+BKM group; and $n = 7$ for the E2+Tam+BKM group). The data are presented as the means ± SEM. $P < 0.001$ (days), $P < 0.001$ (group × days) based on RM ANOVA. $P = \text{n.s.}$ (no significance), shCon/E2+Tam versus shCon/E2+BKM; † $P = 0.019$, shCon/E2+Tam versus shCon/E2+Tam+BKM; ** $P = 0.009$, shMEL/E2+Tam versus shMEL/E2+BKM; *** $P < 0.001$, shMEL/E2+Tam versus shMEL/E2+Tam+BKM (post hoc LSD test).



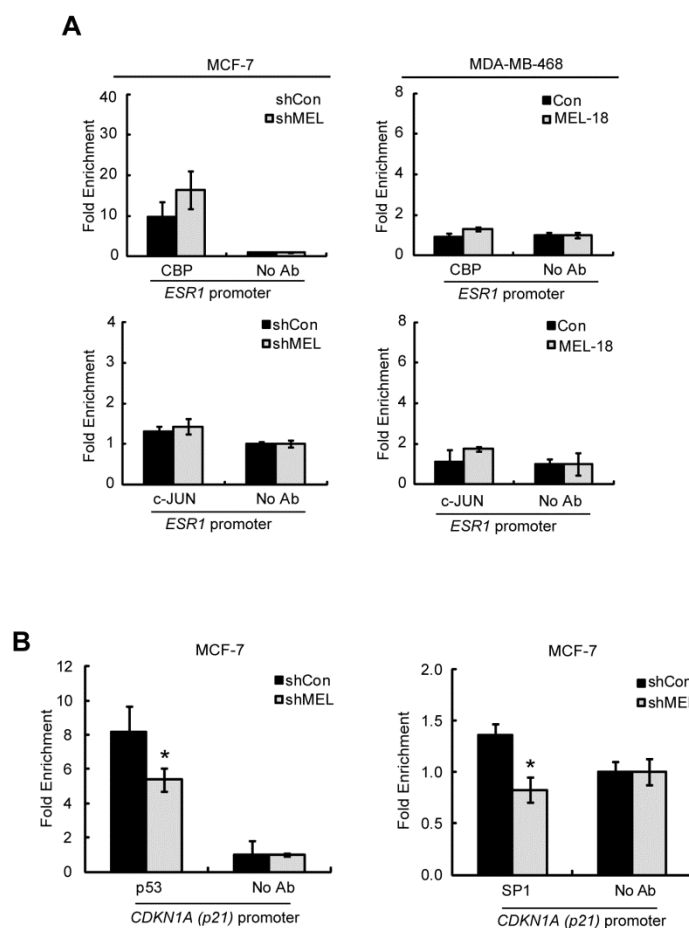
Supplemental Figure 9 Neither the epigenetic status of *ESR1* nor the total expression of *ESR1* transcription factors is affected by MEL-18 expression. **(A)** Immunoblotting (left) and RT-PCR (right) were used to measure the expression of epigenetic modifiers involved in *ESR1* gene regulation in MEL-18-silenced MCF-7 cells. **(B)** ChIP analysis showing the histone modification status and level of recruitment of HDAC1 and DNMT family proteins to the proximal promoter region of *ESR1* in MEL-18-silenced MCF-7 cells. The vertical white lines in the gel images indicate that the lanes were run on the same gel but were noncontiguous. **(C)** Immunoblotting (left) and RT-PCR (right) measuring the expression of PcG proteins in MEL-18-silenced MCF-7 cells and MEL-18-overexpressing MDA-MB-468 cells. Parallel samples examined on separate gels are shown. **GAPDH*, a loading control for RT-PCR **(D)** The expression of *ESR1* transcription factors in the indicated cell lines was examined via immunoblotting. Parallel samples examined on separate gels are shown. The relative immunoblot and RT-PCR band densities are shown at the bottom of each band. The data shown are representative of three independent experiments.



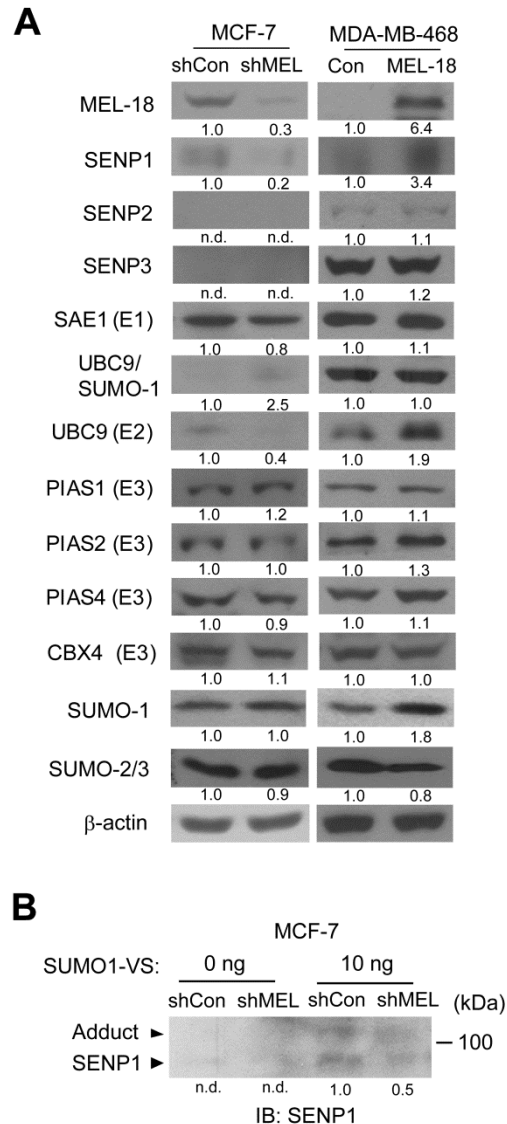
Supplemental Figure 10 MEL-18 is a negative SUMO E3 ligase of p53 but not SP1. (**A** and **B**) Co-immunoprecipitation of 293T cells transfected with pCI-neo (Con) or pCI-neo-MEL-18-FLAG (MEL-18-FLAG) to measure the interaction between MEL-18 and *ESR1* transcription factors. IB, immunoblot. (**C** and **D**) In vitro SUMOylation assay of p53 (**C**) and SP1 (**D**) in the presence or absence of MEL-18. (**E**) In vivo SUMOylation assay of p53 and SP1 in 293T cells co-transfected with the indicated plasmid vectors. The data are representative of three independent experiments.



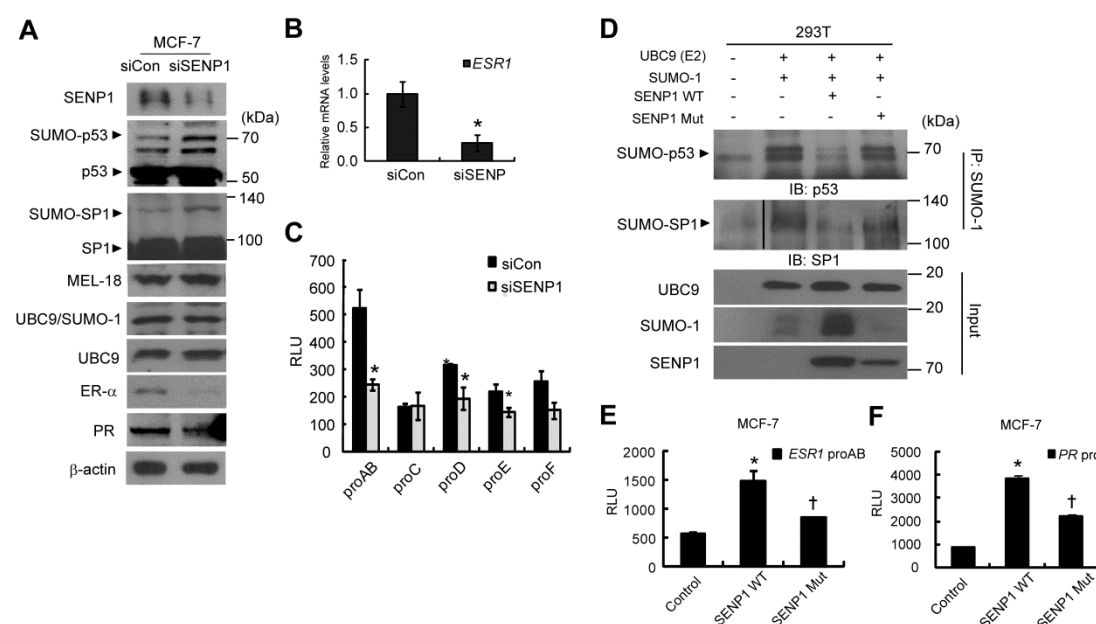
Supplemental Figure 11 The effect of MEL-18 on the SUMOylation of transcription factors and the regulation of their target genes. **(A)** GO analysis of common target genes of MEL-18 and p53/SP1 based on a comparison of two microarray results (our data versus the GSE13291 data). **(B)** MCF-7 cells co-transfected with WT or SUMOylation-deficient mutant constructs of p53 or SP1 and ER pro-Luciferase were subjected to a luciferase reporter assay. * $P < 0.05$ versus Con; † $P < 0.05$ versus WT protein (2-tailed Student's t test). **(C)** Binding of WT p53 and the SUMOylation-deficient p53 K386R mutant to the *ESR1* promoter region. 293T cells were transfected with indicated cDNAs for 48 h and subjected to a ChIP assay. * $P < 0.05$ versus p53 WT (2-tailed Student's t test). The lack of SUMOylation of the p53 K386R mutant was confirmed via immunoblotting. **(D)** The effect of the inhibition of SUMOylation on *ESR1* transcriptional activity in TNBC cells. Cells co-transfected with the *ESR1* promoter construct and MEL-18 cDNA or empty vector were treated with 10 μ M ginkgolic acid (gink) for 24 h and subjected to a luciferase reporter assay. **(E)** To analyze the effect of p53 and SP1 on MEL-18-induced *ESR1* transcription, cells were transfected with the indicated siRNAs, cDNAs and *ESR1* promoter construct for 48 h and subjected to a luciferase reporter assay. * and †, $P < 0.05$ compared to Con and siCon, respectively (2-tailed Student's t test). The data in B-E are presented as the means \pm SD of triplicate experiments.



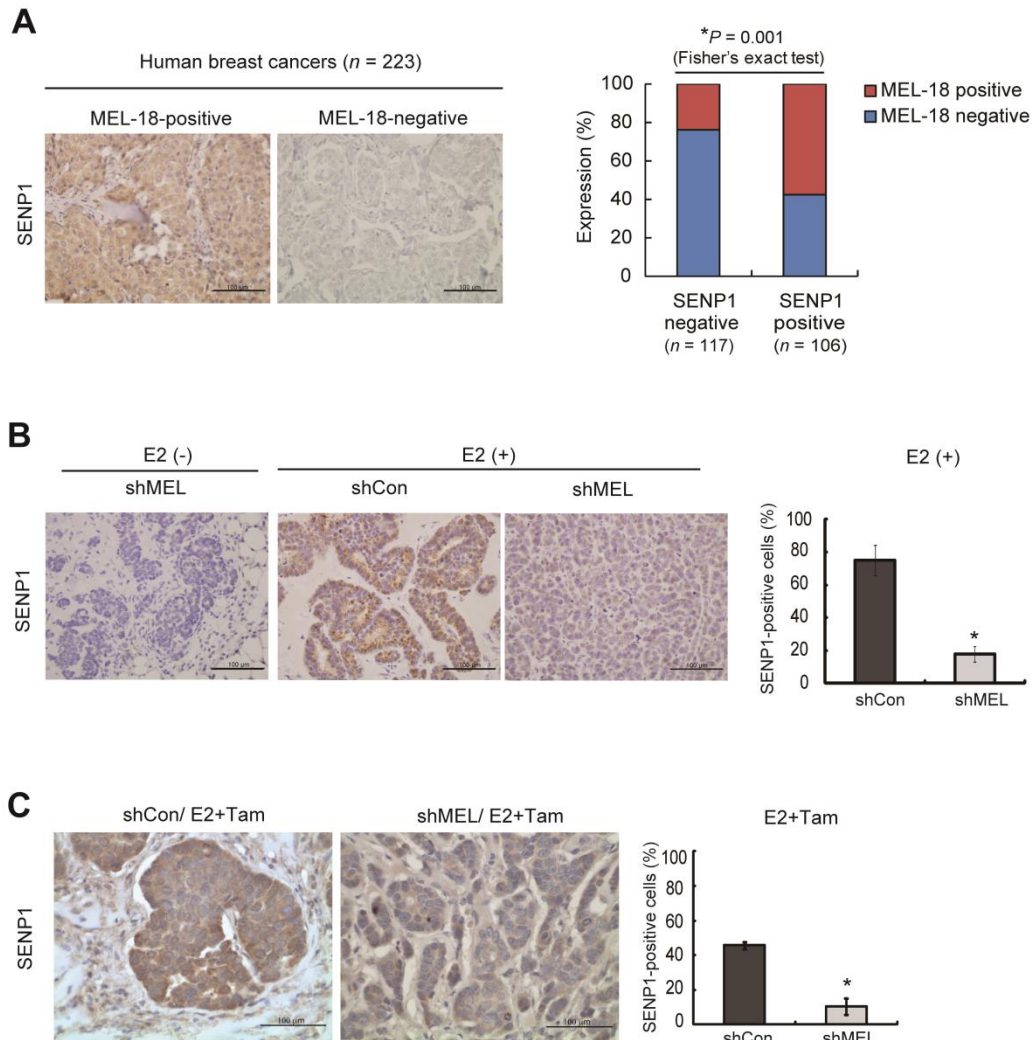
Supplemental Figure 12 The effect of MEL-18 on the binding of transcription factors at their target promoters (**A** and **B**) ChIP analysis showing the enrichment of the indicated proteins in the *ESR1* (**A**) or *CDKN1A* (**B**) promoter region. The data are presented as means \pm SD ($n = 3$). * $P < 0.05$ versus the controls (Con or shCon) based on a 2-tailed Student's t test.



Supplemental Figure 13 The effect of MEL-18 on the expression and activity of SUMOylation/deSUMOylation-regulating factors. **(A)** Immunoblotting of the expression of SUMO-related factors in MEL-18-silenced (left) and MEL-18-overexpressing (right) cell lines. Parallel samples examined on separate gels are shown. **(B)** The effect of MEL-18 expression on the deSUMOylation activity of SENP1. For the in vitro deSUMOylation assay, the lysates from the control and MEL-18-silenced MCF-7 cells were incubated with HA-SUMO-1-VS as described in the Methods section, and the samples were subjected to immunoblotting using the SENP1 antibody. The data are representative of three independent experiments.



Supplemental Figure 14 The expression and enzymatic activity of SENP1 are crucial for the regulation of *ESR1* and PR transcription. (A-C) Immunoblotting (A), qRT-PCR (B) and luciferase reporter assays (C) were performed to measure ER- α expression levels in MCF-7 cells transfected with non-targeted (siCon) or SENP1 siRNA (siSENP1) for 48 h. For immunoblotting for SUMOylated p53 and SP1, cell lysates were prepared following treatment with 20 mM NEM. Parallel samples examined on separate gels are shown in (A). The data are presented as means \pm SD ($n = 3$). * $P < 0.05$ versus siCon (2-tailed student's t test). (D) In vivo SUMOylation assay for p53 and SP1 in 293T cells transfected with the FLAG-SENP1 WT (SENP1 WT) or catalytically inactive mutant SENP1 (SENP1 Mut) vector. The black dividing line in the blot indicates that the lanes were from the same gel but were noncontiguous. (E and F) Assays of *ESR1* and *PR* promoter activity in MCF-7 cells transiently transfected with the WT or mutant SENP1 plasmid (right). The data are presented as means \pm SD ($n = 3$). * and †, $P < 0.05$ versus control and WT SENP1, respectively (2-tailed Student's t test).



Supplemental Figure 15 The effect of MEL-18 on SENP1 expression in clinical specimens and xenografts in vivo. **(A)** Representative IHC images of SENP1 staining (left) and bar graphs showing the correlation between MEL-18 and SENP1 expression (right) in 223 human breast tumors. Scale bars: 100 μm . $*P < 0.05$ (Fisher's exact test). **(B)** The expression status of SENP1 in NOD/SCID mice transplanted with control (shCon) or MEL-18-silenced (shMEL) MCF-7 cells in the presence or absence of E2 administration as determined by IHC. **(C)** IHC analysis for SENP1 in the indicated samples from NOD/SCID mice administered tamoxifen for 4 wk. The data in B and C are presented as means \pm SD ($n = 3$ mice). Scale bars: 100 μm .

Supplemental Table 1. Correlation between clinicopathological characteristics and MEL-18 expression in human breast cancer patients (*n* = 223)

Clinicopathological characteristics	<i>n</i>	MEL-18 expression		<i>P</i> value (Fisher's exact test)
		Negative	Positive	
AJCC stage				0.021
Stage I-II	164	91 (55.5%)	73 (44.5%)	
Stage III-IV	59	43 (72.9%)	16 (27.1%)	
Tumor size				0.001
< 5 cm	117	58 (49.6%)	59 (50.4%)	
> 5 cm	106	76 (71.7%)	30 (28.3%)	
Lymph node metastasis				0.497
Negative	119	69 (58.0%)	50 (42.0%)	
Positive	104	65 (62.5%)	39 (37.5%)	
Histological grade*				0.098
Grade 1-2	138	81 (58.7%)	57 (41.3%)	
Grade 3	54	39 (72.2%)	15 (27.8%)	
ER- α status				0.001
Negative	97	70 (72.2%)	27 (27.8%)	
Positive	126	64 (50.8%)	62 (49.2%)	
PR status				0.029
Negative	103	70 (68.0%)	33 (32.0%)	
Positive	120	64 (53.3%)	56 (46.7%)	
HER2 status (IHC)				0.164
Negative	181	113 (62.4%)	68 (37.6%)	
Positive	42	21 (50.0%)	21 (50.0%)	
Molecular classification**				0.003
Luminal	125	64 (51.2%)	61 (48.8%)	
HER2-positive	29	16 (55.2%)	13 (44.8%)	
Triple-negative	53	45 (84.9%)	8 (15.1%)	

*Invasive ductal carcinoma only.

**Based on the ER- α , PR, and HER2 status.

Supplemental Table 2. The effect of MEL-18 knockdown on estrogen-independent T47D tumor formation in vivo ($n = 8$)

Group	Tumor incidence ($n = 8$)						
	Day 7	Day 15	Day 22	Day 29	Day 36	Day 43	Day 52
shCon	0 / 8 (0%)	0 / 8 (0%)	0 / 8 (0%)	1 / 8 (12.5%)	2 / 8 (25%)	2 / 8 (25%)	2 / 8 (25%)
shMEL	0 / 8 (0%)	1 / 8 (12.5%)	2 / 8 (25%)	6 / 8 (75%)	7 / 8 (87.5%)	7 / 8 (87.5%)	7 / 8 (87.5%)
<i>P</i> value	< 0.0001						

Tumor incidence in NOD/SCID mice injected with T47D cells expressing either control (shCon) or MEL-18 shRNA (shMEL) in the absence of E2 injection. The significance of the differences was determined via Poisson distribution analysis.

Supplemental Table 3. Correlation between clinicopathological characteristics and SENP1 expression in human breast cancer patients ($n = 223$)

Clinicopathological characteristics	<i>n</i>	SENP1 expression		<i>P</i> value (Fisher's exact test)
		Negative	Positive	
AJCC stage				0.649
Stage I-II	164	88 (53.7%)	76 (46.3%)	
Stage III-IV	59	29 (49.2%)	30 (50.8%)	
Tumor size				0.032
< 5 cm	117	53 (45.3%)	64 (54.7%)	
> 5 cm	106	64 (60.4%)	42 (39.6%)	
Lymph node metastasis				0.350
Negative	119	66 (55.5%)	53 (44.5%)	
Positive	104	51 (49.0%)	53 (51%)	
Histologic grade*				0.010
Grade 1-2	138	66 (47.8%)	72 (52.2%)	
Grade 3	54	37 (68.5%)	17 (31.5%)	
ER- α status				<0.001
Negative	97	64 (66.0%)	33 (34.0%)	
Positive	126	53 (42.1%)	73 (57.9%)	
PR status				0.080
Negative	103	61 (59.2%)	42 (40.8%)	
Positive	120	56 (46.7%)	64 (53.3%)	
HER2 status (IHC)				0.735
Negative	181	94 (51.9%)	87 (48.1%)	
Positive	42	23 (54.8%)	19 (45.2%)	
Molecular classification**				0.001
Luminal	125	53 (42.4%)	72 (57.6%)	
HER2-positive	29	17 (58.6%)	12 (41.4%)	
Triple-negative	53	37 (69.8%)	16 (30.2%)	

*Ductal type only.

**Based on the ER- α , PR, and HER2 status.

Supplemental Table 4. Univariate and multivariate analyses of breast cancer patient survival

	Univariate			Multivariate		
	HR	95% CI	<i>P</i> value	HR	95% CI	<i>P</i> value
DFS						
Stage (I or II vs. III or IV)	3.917	2.247-6.831	< 0.001	3.692	1.557-8.751	0.003
Grade (1 or 2 vs. 3)	0.979	0.504-1.900	0.949			
LN metastasis	2.33	1.307-4.152	0.004	1.051	0.429-2.578	0.913
ER- α (Negative vs. Positive)	0.566	0.324-0.989	0.046	0.683	0.384-1.214	0.194
PR (Negative vs. Positive)	0.692	0.397-1.206	0.194			
HER2 (Negative vs. Positive)	0.951	0.462-1.957	0.891			
SENP1 (Negative vs. Positive)	0.581	0.323-1.043	0.069	0.595	0.327-1.083	0.089
OS						
Stage (I or II vs. III or IV)	4.874	2.406-9.876	< 0.001	7.346	2.126-25.376	0.002
Grade (1 or 2 vs. 3)	1.001	0.443-2.260	0.998			
LN metastasis	2.386	1.150-4.949	0.019	0.590	0.164-2.123	0.419
ER- α (negative vs. positive)	0.509	0.251-1.031	0.061			
PR (Negative vs. positive)	0.528	0.261-1.071	0.077			
HER2 (negative vs. positive)	0.821	0.316-2.133	0.686			
SENP1 (negative vs. positive)	0.722	0.353-1.478	0.373	0.688	0.336-1.409	0.306

*Cox regression hazard model.

HR = hazard ratio; CI = confidence interval.

Supplemental Methods

Patients and surgical specimens. For survival analyses, 223 consecutive patients with breast cancer who successfully underwent surgery at Hanyang University Hospital (Seoul, Korea) between January 2000 and December 2005 were enrolled. Histopathological and clinical data, including patient's age, histologic type, tumor grade, tumor size, lymph node status, AJCC stage, ER- α and PR status, HER2 status, information regarding adjuvant chemotherapy, radiotherapy and endocrine treatment, and follow-up data, were obtained from pathology reports and medical records. All cases were primary and sporadic and were untreated before surgery. The patient sample was homogeneous with respect to surgical procedures, postoperative therapy, and follow-up schedule. Most patients received modified radical mastectomy or breast-conserving surgery with or without axillary lymph node dissection followed by adjuvant chemotherapy and/or hormonal therapy. The low-risk group of patients with stage I cancer who were positive for hormone receptors received only tamoxifen treatment after surgery. Patients with stage I (high-risk group) or II received adriamycin and cyclophosphamide (AC) or cyclophosphamide, methotrexate, and 5-fluorouracil (CMF) chemotherapy. Patients with stage III cancer received AC and paclitaxel chemotherapy. Adjuvant hormonal therapy with tamoxifen was administered after chemotherapy to patients exhibiting a positive ER- α status. Radiation therapy was performed on patients with stage III or stage II tumors greater than 5 cm in diameter. The mean follow-up duration was 75.7 months, during which 32 (14.3%) patients died and 191 (85.7%) patients survived.

Tissue microarray construction and IHC staining. Hematoxylin and eosin-stained slides from formalin-fixed, paraffin-embedded tissue blocks were used to define the most morphologically representative and non-necrotic areas. Single-tissue cores (2 mm in diameter) were sampled from each paraffin block and assembled into a recipient paraffin block using a

tissue microarray (TMA) instrument (AccuMax array, ISU ABXIS). Tissue sections with a thickness of 4 μ m were sliced and deparaffinized. Immunostaining was performed using a Bond Max automated immunostainer (Vision BioSystems). Heat-induced epitope retrieval was performed using Bond Epitope Retrieval Solution. Endogenous peroxidase activity was blocked with 0.3% hydrogen peroxide. The sections were stained using primary antibodies against MEL-18 (dilution 1:50, sc-10744; Santa Cruz Biotechnology) and SENP1 (dilution 1:200, AP1230; Abgent) for 15 min at room temperature. The slides were incubated in post-primary reagent for 15 min at room temperature. The reactions were developed using BOND Polymer Refine Detection reagent followed by colorimetric development using 3,3'-diaminobenzidine tetrahydrochloride (DAB; Sigma-Aldrich) as the chromogen. MEL-18 and SENP1 immunoreactivity was evaluated by two pathologists in a blinded manner. The German semi-quantitative scoring system was used to quantify the staining intensity and area. For each sample, a score was assigned based on the percentage of positively stained cells as follows: no stained cells, 0 points; 1 to 24% stained cells, 1 point; 25 to 49% stained cells, 2 points; 50 to 74% stained cells, 3 points; and 75 to 100% stained cells, 4 points. Another score was assigned based on the staining intensity as follows: negative staining, 0 points; weak staining, 1 point; moderate staining, 2 points; and strong staining, 3 points. A final score was obtained by multiplying the two scores. If the final score was 4 or higher, the expression status was considered positive.

Plasmids and siRNAs. FLAG-tagged MEL-18 cDNA and approximately 1 kb MEL-18 promoter were generated by PCR and inserted into pCI-neo vector (Promega) and pGL3 luciferase reporter vector (Promega), respectively. ER- α cDNA and ERE luciferase construct were gift from Incheol Shin (Hanyang University, Seoul, Korea; ref. 5). The *ESR1* promoter reporter constructs ER proAB, proC, and proD in pGL3-basic vector, were kindly provided by Shin-Ichi Hayashi (Saitama Cancer Center Research Institute, Saitama, Japan; ref. 1). ER proE

and proF (ref. 1) were generated by PCR and cloned into the pGL3 vector. PRE luciferase and pcDNA3-HA-SUMO-1 constructs were obtained from Addgene (Cambridge, MA, USA), deposited by Donald McDonnell (Duke University, Durham, NC, USA; ref. 6) and Junying Yuan (Harvard Medical School, Boston, MA, USA; ref. 7), respectively. FLAG-tagged UBC9 cDNA was gift from Chul Geun Kim (Hanyang University, Seoul, Korea). HA-tagged ubiquitin construct was kindly provided by Moshe Oren (Weizmann Institute of Science, Rehovot, Israel; ref. 8). The RING1B wild type and C51W/C54S mutant constructs (kindly provided by Seongman Kang, Korea University, Seoul, Korea; ref. 9) were inserted into pCI-neo vector. The p53 wild type and SUMOylation-deficient K386R mutant constructs were generated by PCR and mutagenesis, respectively, and cloned into the pCI-neo vector. The SP1 wild type and E18A mutant constructs were kindly provided by Jan-Jong Hung (National Cheng Kung University, Tainan, Taiwan; ref. 10). FLAG-tagged SENP1 wild type or inactive mutant (R630L, K631M) constructs were obtained from Addgene, deposited by Edward Yeh (The University of Texas MD Anderson Cancer Center, Houston, TX, USA; ref. 11). For SENP1 stable expression, the SENP1 wild type cDNA was subcloned into pCI-neo vector. For transient knockdown experiments, a non-targeting siRNA and siRNAs targeting ER- α , BMI-1, p53, Sp1, and SENP1 were purchased from Bioneer Corporation. The SmartPool siRNAs of a control and MEL-18 were obtained from Dharmacon RNA Technologies. These siRNAs were transfected into cells with Lipofectamine 2000 (Invitrogen) for 48 h as described by manufacturers.

Antibodies. Antibodies used for immunoblotting were MEL-18 (sc-10744), ER- α (sc-543), PR (sc-539), HER2 (sc-284), SENP1 (sc-46634), p53 (sc-126), SP1 (sc-59), CBP (sc-369), SUMO-1 (sc-9060), BMI-1 (sc-10745), Geminin (sc-13015), RING1B (sc-101109), EED (sc-28701), YY1 (sc-7341), CBX2 (sc-19297), HA (sc-805), HDAC1 (sc-7872), HDAC2 (sc-7899), DNMT1 (sc-20701), DNMT3a (sc-20703), and pRb2/p130 (sc-317) from Santa Cruz Biotechnology; HER2 (NCL-L-CB11) from Leica Biosystems; TFF1 (12419), EZH2 (3147),

AKT (9272), and Ubiquitin (3936) from Cell Signaling Technology; H3Ac (06-599), H4Ac (06-866), H3K27me3 (07-449), p300 (05-257), and c-JUN (06-225) from Millipore; SUZ12 (ab12073), CBX7 (ab21873), H3K9me3 (ab8898), and p-AKT Ser473 (ab66138) from Abcam. SAE1 (AP1199), UBC9 (AP1064), SUMO2/3 (AP1224), PIAS1 (AB1243), PIAS2 (AP1246), PIAS4 (AP1249), CBX4 (AP2514), SENP2 (AP1232) and SENP3 (AP1234) from Abgent; β -actin from Sigma-Aldrich.

Primers. Primers used for RT-PCR and qRT-PCR were: *MEL-18 (PCGF2)*, 5'-GGCGGGATTCTATGCAG-3' and 5'-AATTCGATGGAGAGGCTGAC-3'; *ESR1*, 5'-ACCATGACCCTCCACACCAAAGCATC-3' and 5'-GTAGTTGTACACGGCGGGCTTGCTG-3'; *TFF1 (pS2)*, 5'-GTACACGGAGGCCAGACAGA-3' and 5'-AGGGCGTGACACCAGGAAA-3'; *PR*, 5'-GGCCATACCTATCTCCCTGGA-3' and 5'-CTCCACGTCCGACAGCGACT-3'; *SENPI1*, 5'-ACTGATAGTGAAGATGAATTCCTGA-3' and 5'-CATCCTGATTCCCATTACGAA-3'; *GAPDH*, 5'-CATGTTCCAATATGATTCCA-3' and 5'-CCTGGAAGATGGTGATG-3'; *HDAC1*, 5'-GGAAATCTATCGCCCTCACA-3' and 5'-CTCGGACTTCTTTGCATGGT-3'; *HDAC2*, 5'-GAGGTGGCTACACAATCCGT-3' and 5'-TTCGACCTCCTTCTCCTTCA-3'; *EP300 (p300)*, 5'-AAACCCACCAGATGAGGAC-3' and 5'-TATGCACTAGATGGCTCCGCAG-3'; *DNMT1*, 5'-ATGGCAGATGCCAACAGCCCC-3' and 5'-CTCCTTCAGTTTCTGTTTGGGTG-3'; *DNMT3A*, 5'-GGGGACGTCCGCAGCGTCACAC-3' and 5'-CAGGGTTGGACTCGAGAAATCGC-3'; *SUV39H1*, 5'-GGAGAAAGATGGCGGAAA-3' and 5'-GACAAGAAAGCTTGGCTAGT-3'; *RBL2 (pRB2/p130)*, 5'-GAGCTGTGCAGCCGCCTCAA-3' and 5'-GGCTGTCGCCGCTGTTTCCT3'.

Viral infection and stable transfection. For stable MEL-18 overexpression or knockdown, lentiviral MEL-18 shRNA-infected cell lines and retroviral MEL-18-overexpressing cell lines,

respectively, were established as previously described (12, 13). To inhibit RING1B activity or restore SENP1 expression in MEL-18-silenced MCF-7 cells, the cells were transfected with pCI-neo, pCI-neo-RNF2 C51W/C54S, or pCI-neo-SENP1 vector and selected using 1 mg/ml G418 sulfate (Sigma-Aldrich).

Immunoblotting and immunoprecipitation. Cells were lysed in radioimmunoprecipitation assay (RIPA) buffer. To detect SUMOylated proteins, cells were extracted in RIPA buffer containing 20 mM N-ethylmaleimide (NEM, Sigma-Aldrich) and sonicated. Immunoblotting was performed as previously described (12). For co-immunoprecipitation, lysates of 293T cells transfected with pCI-neo or pCI-neo-MEL-18-FLAG vector were immunoprecipitated using an anti-p53 or anti-FLAG antibody. The precipitates were analyzed via immunoblotting as described above. The immunoblot band densities were determined using AlphaEase FC Software (AlphaInnotech) and normalized to the expression of the protein β -actin.

Reverse-transcription (RT)-PCR and quantitative real-time (qRT)-PCR. Total RNA isolation and RT-PCR were performed as previously described (12). To quantify the RNA expression levels, qRT-PCR was performed using the 7300 Real-Time PCR System and SYBR Green Master Mix (Applied Biosystems). These data were normalized to the expression of the housekeeping gene GAPDH.

Luciferase reporter assay. For the luciferase reporter assay, cells were seeded on a 12-well plate and transfected with reporter constructs and a β -gal expression vector for 24 h or 48 h. Then, luciferase reporter assays were performed as previously described (14).

Cell proliferation assay. The effect of MEL-18 on breast cancer cell growth upon tamoxifen treatment was investigated using a (3-(4,5-dimethylthiazol-2-yl)-2,5-

diphenyltetrazolium bromide (MTT) assay kit (Promega) as described previously (12). Briefly, cells were seeded on 96-well plates and treated with ethanol or tamoxifen. After 5 d of treatment, the cells were incubated in MTT dye solution at 37°C for 3 h, and the reaction was terminated via the addition of solubilization/stop solution. The absorbance at 570 nm was measured using a microplate reader.

Supplemental References

1. Kos M, Reid G, Denger S, and Gannon F. Minireview: genomic organization of the human ERalpha gene promoter region. *Mol Endocrinol.* 2001;15(12):2057-63.
2. Macaluso M, Montanari M, Noto PB, Gregorio V, Bronner C, and Giordano A. Epigenetic modulation of estrogen receptor-alpha by pRb family proteins: a novel mechanism in breast cancer. *Cancer Res.* 2007;67(16):7731-7.
3. Shirley SH, Rundhaug JE, Tian J, Cullinan-Ammann N, Lambertz I, Conti CJ, and Fuchs-Young R. Transcriptional regulation of estrogen receptor-alpha by p53 in human breast cancer cells. *Cancer Res.* 2009;69(8):3405-14.
4. deGraffenried LA, Hilsenbeck SG, and Fuqua SA. Sp1 is essential for estrogen receptor alpha gene transcription. *J Steroid Biochem Mol Biol.* 2002;82(1):7-18.
5. Park S, Song J, Joe CO, and Shin I. Akt stabilizes estrogen receptor alpha with the concomitant reduction in its transcriptional activity. *Cellular signalling.* 2008;20(7):1368-74.
6. Giangrande PH, Kimbrel EA, Edwards DP, and McDonnell DP. The opposing transcriptional activities of the two isoforms of the human progesterone receptor are due to differential cofactor binding. *Molecular and cellular biology.* 2000;20(9):3102-15.
7. Terui Y, Saad N, Jia S, McKeon F, and Yuan J. Dual role of sumoylation in the nuclear localization and transcriptional activation of NFAT1. *The Journal of biological chemistry.* 2004;279(27):28257-65.
8. Minsky N, and Oren M. The RING domain of Mdm2 mediates histone ubiquitylation and transcriptional repression. *Molecular cell.* 2004;16(4):631-9.
9. Lee SJ, Choi JY, Sung YM, Park H, Rhim H, and Kang S. E3 ligase activity of RING finger proteins that interact with Hip-2, a human ubiquitin-conjugating enzyme. *FEBS letters.* 2001;503(1):61-4.
10. Wang YT, Chuang JY, Shen MR, Yang WB, Chang WC, and Hung JJ. Sumoylation of

specificity protein 1 augments its degradation by changing the localization and increasing the specificity protein 1 proteolytic process. *Journal of molecular biology*. 2008;380(5):869-85.

11. Cheng J, Kang X, Zhang S, and Yeh ET. SUMO-specific protease 1 is essential for stabilization of HIF1alpha during hypoxia. *Cell*. 2007;131(3):584-95.
12. Lee JY, Jang KS, Shin DH, Oh MY, Kim HJ, Kim Y, and Kong G. Mel-18 negatively regulates INK4a/ARF-independent cell cycle progression via Akt inactivation in breast cancer. *Cancer Res*. 2008;68(11):4201-9.
13. Park JH, Lee JY, Shin DH, Jang KS, Kim HJ, and Kong G. Loss of Mel-18 induces tumor angiogenesis through enhancing the activity and expression of HIF-1alpha mediated by the PTEN/PI3K/Akt pathway. *Oncogene*. 2011;30(45):4578-89.
14. Qian T, Lee JY, Park JH, Kim HJ, and Kong G. Id1 enhances RING1b E3 ubiquitin ligase activity through the Mel-18/Bmi-1 polycomb group complex. *Oncogene*. 2010;29(43):5818-27.